29th Congress of the International Council of the Aeronautical Sciences
St. Petersburg, Russia; September 7-12, 2014

LEE-SIDE FLOW SIMULATIONS OF CRUCIFORM WING-BODY CONFIGURATIONS AT INCOMPRESSIBLE MACH NUMBERS

Janine Versteegh* **
***University of the Witwatersrand**
****Council for Scientific and Industrial Research (CSIR)**
jversteegh@csir.co.za

Keywords: *slender bodies, strakes, engineering methods, FVM, DVM*

Abstract

The lee-side flow was simulated for a circular wing-body combination with very low aspect ratio wings in the '+' (plus) configuration at incompressible speeds. Two 2D engineering level methods, the discrete vortex model (DVM) and free vortex model (FVM) methods were utilized to simulate the flow for three different span to body diameter ratios, namely 1.25, 1.50 and 1.75. The results were compared to experimentally validated computational fluid dynamics (CFD) data in order to investigate the applicability of the two methods in predicting the aerodynamic loads as well as the vortex shedding. A comparison of the normal force and centre-of-pressure indicated that the DVM method correlates well with the CFD loads, whereas the FVM method is less suitable for span to body diameter ratios above 1.25.

Nomenclature

a	Body outer radius (m)
C_N	Normal force coefficient
C_m	Moment coefficient
D	Body outer diameter (m)
M	Free stream Mach number
K_{W_B}	Body-on-wing carry-over factor
K_{B_W}	Wing-to-body carry-over factor
k	Convergence factor
s_m	Wing span (m)
t	Time (s)
V	Free stream velocity (m/s)
v	Complex velocity potential in the y-direction
w	Complex velocity potential in the z-direction
x_{C_p}	Centre-of-pressure position = $\frac{C_m}{C_N}$ (calibers)
y	Lateral vortex position (m)
z	Vertical vortex position (m)
α	Angle of attack (°)
ϕ	Velocity potential

1 Introduction

The flow features in the lee side of slender bluff bodies have been the subject of investigations for decades. Engineering level methods, which are vital during the preliminary design phases, have been developed for slender bodies and body-wing configurations (generally with aspect ratios limited to a range of 0.25 to 4). All engineering level methods to date are based on slender body theory, which does not predict any Mach number dependency. The more frequent use of very low aspect ratio wings have emerged in recent decades, revealing the limitations of existing methods in predicting the flow field topologies of configurations with low span to body diameter ratios (s_m/D) and wings of very low aspect ratio. This class of configuration has been recently studied at supersonic speeds [1][2][3][4].

The free vortex model (FVM) method was developed in 2013 [4] for a tangent ogive missile with very low aspect ratio wings

(hereafter referred to as strakes). The method used a two-dimensional unsteady flow method to predict the lee side flow over the missile at supersonic speeds with strakes in the '+' orientation. While accurately predicting vortex positions and normal force at supersonic speeds and low to moderate angles of attack, limitations were observed in the prediction of the centre-of-pressure positions. In this study the applicability of the method to subsonic, incompressible flow is examined, thereby assessing the methods across the speed range and the limitations of the slender body theory assumptions inherent in the methods for very low aspect ratio wings.

Along with the FVM method, the discrete vortex model (DVM) method was also included in the investigation. The FVM and DVM predictions were compared to experimentally validated computational fluid dynamics (CFD) data in order to determine the accuracy of the predictions.

2 Configuration

The configuration relevant to this study is based on the configuration used in references [1] to [4] with the addition of two span to body diameter ratios (s_m/D). The three different s_m/D ratios are thus 1.25, 1.50 and 1.75. The configurations all consist of a 3 caliber tangent ogive nose with a total forebody length of 4.75 calibers. The strakes are 11.25 calibers in length with the total body length of 19 calibers. The general dimensions can be seen in Fig. 1.

3 Engineering Methods

3.1 Component Build-up Method

In this study, the method for calculating the normal force over the entire configuration is based on the component build-up method. This allows the comparison to the total loads that are obtained from CFD simulations as well as experimental testing owing to the fact that the normal force obtained from the DVM and FVM methods is the component due to the vortex separation.

Each configuration may be divided into three parts: the forebody section, cruciform wing-body section and the aft body section. Each of these sections generates a normal force component that equals the total normal force when summed. Utilizing the method of Allen [5], the normal force for cruciform wing-body section is expressed as the sum of components, namely the load due to an attached potential flow and a vortex induced load. The total normal force is then

$$C_N = C_{N_{fore\,body}} + C_{N_{attached}} + C_{N_{vortex}} + C_{N_{aft\,body}} \quad (1)$$

The attached potential component is given as [3]

$$C_{N_{attached}} = \left(K_{W_B} + K_{B_W}\right) C_{N_{W_a}} \sin\alpha \cos\left(\frac{\alpha}{2}\right) \quad (2)$$

Where $C_{N_{W_a}}$ is the rate of change of the wing alone normal force at $\alpha = 0$.Therefore the total load can be expressed as

$$C_N = C_{N_{fore\,body}} + \left(K_{W_B} + K_{B_W}\right) C_{N_{W_a}} \sin\alpha \cos\left(\frac{\alpha}{2}\right) + C_{N_{vortex}} + C_{N_{aft\,body}} \quad (3)$$

The vortex load $C_{N_{vortex}}$ is then determined using the DVM and FVM methods and the accuracy with which it is predicted is the topic of this study. The forebody and aft-body components were obtained from the validated CFD simulations.

3.2 Two-dimensional Theory

The methods considered are based on the theoretical concept that a three-dimensional, steady, compressible flow problem can be reduced to a time dependent, two-dimensional, incompressible flow problem [3][7]. This simplification reduces the computing time of the engineering method and allows incompressible potential flow equations to be used. Assuming

an impulsively started flow in the y-z plane (see Fig.1), the potential flow equation reduces to

$$\phi_{\bar{y}\bar{y}} + \phi_{\bar{z}\bar{z}} \tag{4}$$

This method of reducing a three-dimensional problem to a two-dimensional problem exists under the assumption that the body diameter is constant (or changes slowly) in the direction perpendicular to the plane considered or $M \approx 1$. The physical axes system with the wing-body cross section is transformed to a circle plane in order to perform the analysis. The transformation follows that of references [3], [6] and [7]. It was also shown that the equations of the rate of change for the jth vortex with respect to the axial positions are

$$\frac{dy_j}{dt} = v_j \frac{1}{V \cos \alpha} \tag{5}$$

$$\frac{dz_j}{dt} = w_j \frac{1}{V \cos \alpha} \tag{6}$$

3.3 Discrete Vortex Model

In this method, the vortex sheet that separates from the strake side edge is represented by multiple discrete singularities (vortex filaments). The shed vortices are then modeled as free vortices which then move as Langrangian fluid particles [3]. In order to define the shed vortex it is required to first determine its initial position in two orthogonal directions (generally in the y-z plane) as well as the strength of the vortex. The nature of the strake side edge is defined by the Kutta-Joukowski condition and the local velocity at the edge is determined from the velocity potential. The method for predicting the path of the discrete vortices is elucidated by references [3] and [8].

3.4 Free Vortex Model

The FVM model uses the tracking of shed concentrated vortices along the strake edges (i.e. one per strake), rather than vortex filaments, to determine the position of the vortices along the length of the strakes. The vortex strength is also determined and, together with the vortex positions, is used to calculate the normal force and centre-of-pressure induced by the vortex sheet. This is accomplished using the vortex impulse theorem. Also, the Kutta condition is not satisfied at any stage in the FVM solution method. The set of differential equations to be solved require an initial vortex position and strength [4]. Contrary to other engineering methods, the FVM method does not assume a constant vortex strength but determines the vortex positions using the shed vorticity. A detailed explanation of the development of the FVM method is described in references [4] and [10].

4 Computational Fluid Dynamics

A global loads andflow field database was compiled using CFD. A symmetric computational model was constructed assuming that no asymmetric vortices are expected at such low speeds. The flow domain modeled extended to 100 times the length of the missile in all directions. Mesh independent results were obtained with a structured mesh of 22 million cells. In order to accurately capture the nature of the vortices and their effects on the aerodynamic loads, the meshed volume containing the lee-side flow and shed vortices was refined so that the vortex core consisted of at least 8 cells (in the cross-flow planes).

The CFD simulations were performed using ANSYS Fluent v15, implementing a coupled pressure-velocity algorithm with second order upwind spatial discretization scheme. The Spalart-Allmaras model was used as it is specifically designed for aerospace applications and external aerodynamics. Simulations were run on 48 nodes taking approximately 20 CPU hours. The solutions were considered converged when the residuals had reduced by a third order of magnitude and the loads asymptoted to constant values. The simulations were run at a Mach number of 0.1 and angles of attack from 0° to 25°.

5 Experimental Validation

Due to the complex nature of the lee-side flow associated with missile-type configurations, the CFD simulations were validated experimentally

in the Low Speed Wind Tunnel (LSWT) of the Council for Scientific and Industrial Research (CSIR). The LSWT is a subsonic, closed loop wind tunnel with an atmospheric test section – this is accomplished by an atmospheric slot just aft of the test section. Tests were conducted at three Mach numbers namely 0.1, 0.2 and 0.3. The Reynolds numbers based on body diameter at each Mach number are 8.87×10^4, 1.74×10^5 and 2.54×10^5 respectively for a 45mm diameter model.

The loads of interest, normal force and pitching moment, were measured up to an angle of attack of 20°. The maximum pitch angle was restricted to 20° due to the physical constraints of the model support structure (see Fig. 2). The angle of attack range at Mach 0.3 was reduced to 16° due to the presence of increased model vibration and grounding at higher angles of attack. The uncertainty$\Delta C_N$for the experimental data, based on a coverage factor of k=2, is 0.66, 0.16 and 0.07 for Mach numbers 0.1, 0.2 and 0.3 respectively. The results for the three configurations are shown in Figs. 3 to 5.

The CFD simulations correlate well with the available experimental data. However, for s_m/D of 1.25, there is a measurable discrepancy between the experimental and CFD normal force at 20° angle of attack. From these results it was established that the CFD simulations predicted the lee side flow accurately and can be used as a reference for comparisons with the engineering prediction methods. Also notice that the experimental normal force indicates no Mach number dependence. The centre-of-pressure positions also show no dependence on Mach number above angles of attack of 6°. The discrepancies below 6° have been attributed to the large increase in uncertainty at very low loads. For Mach 0.1, 0.2 and 0.3 the uncertaintiesΔx_{C_p}at these low angles are approximately11.8, 5.3 and 2.5 respectively. At angles of attack above 6°,Δx_{C_p}reduces to 2, 0.2, and 0.1 for Mach 0.1, 0.2 and 0.3 respectively. Since no Mach number dependency is expected at low angles, it was concluded that the experimental$x_{C_p}$is best represented by the Mach 0.3 data.

6 FVM and DVM Results

6.1 Load Predictions

The comparisons of normal force and centre-of-pressure for the three s_m/D configurations are shown in Figs. 6 to 8. It should be noted that the FVM and DVM methods do not predict any Mach number dependency [3][4]. The configuration with s_m/D=1.25, it can be seen in Fig. 6 that the FVM method over-predicts the normal force above an angle of attack of 6°. Although the slight decrease in slope above 15° also decreases the error between the FVM and CFD predictions up to 25° angle of attack. The maximum deviation for the FVM method occurs at 6° angle of attack, with a 19% higher value than the CFD normal force. The normal force is slightly under-predicted by the DVM method for angles of attack below 15° with a maximum deviation of 31% at 4°. The centre-of-pressure (in calibers) is reasonably well predicted below 4° angle of attack by both the FVM and DVM methods. Above 6° both the FVM and DVM methods predict the centre-of-pressure to be further forward toward the nose of the body with the FVM showing better correlation with the CFD simulations.

In Fig. 7, for the s_m/D=1.5configuration, it may be observed that both the FVM and DVM methods under-predict the normal force compared to the CFD data above 10° angle of attack. Below 10° the FVM method over-predicts the normal force with the largest error of15% at 1°. The DVM method under-predicts the normal force by 27% at very low angles of attack, although the centre-of pressure position is well predicted at these angles. Above 6° angle of attack the centre-of-pressure positions are predicted further forward by both methods by an almost constant offset, the FVM model having the smallest overall error.

Up to 15° angle of attack, the FVM method predicted normal force for s_m/D=1.75 correlates well with the CFD data. Above this there is a sudden decrease in the C_N-α slope, which is also present at s_m/D=1.5 (see Figs. 7 and 8). The centre-of-pressure is predicted further aft of the body compared to CFD for the very low angles by both FVM and DVM methods. As with the

other configurations the centre-of-pressure positions are predicted further forward by both methods above 6° angle of attack. Here the FVM method shows better correlation in terms of absolute values, although the x_{C_p}-α slope better from that of the CFD data.

6.2 Vortex positions

For the s_m/D=1.25 configuration the FVM method predicts vertical positions of vortices further away from the body as compared to the CFD. In contrast the DVM method predicts the vertical vortex positions much closer to the body. The lateral vortex positions are very well predicted by the FVM method whereas the DVM method here predicts the lateral vortex positions further away from the body.

For both the s_m/D=1.5 and 1.75 configurations the FVM method predicts the vertical vortex positions much further away from the body. The vertical vortex positions are well predicted by the DVM method if predicted slightly lower for the s_m/D=1.5 configuration. For both configurations the FVM method predicts the lateral vortex positions to be much closer to the body compared to CFD and the DVM method much further away from the body. These results are demonstrated in Figs. 9 to 11 at an angle of attack of 10° which are typical for the angles assessed.

7 Discussion

7.1 FVM Method

Overall, the FVM method predicts the loads and vortex positions well for the s_m/D=1.25 configuration and less so for the two higher s_m/D configurations. In references [4] and [10] the FVM method was applied to three different supersonic speeds namely Mach 2, 2.5 and 3. For the s_m/D=1.25 configuration (Case A in reference [4]) as presented in this study the normal force is predicted very well by the FVM method up to 10° angle of attack for all Mach numbers considered. At angles above 15° the loads are under-predicted with errors less than 10%. For the incompressible speeds presented in this study the FVM method over-predicts the normal force by an error of 19% or less at all angles of attack. The FVM predictions at supersonic speeds are poorer, predicting the centre-of-pressure positions further aft at the angles of attack below 10° and further forward above 10°.

The vortex positions are very well predicted by the FVM method when applied at supersonic speeds, whereas the subsonic predictions are poorer predicting the vortices slightly further away from the body in the vertical direction.

The investigation by references [1] and [4] did not include configurations with span to body diameter ratios larger than 1.25. In this study it was shown that the accuracy with which the FVM method predicts the loads deteriorates as the span to body diameter ratio increases. The vortex positions are also poorly predicted at the higher span to body diameter ratios.

7.2 DVM Method

In reference [10] the DVM method (with no secondary vortex predictions) was applied to supersonic Mach numbers. It was shown that the normal force was over-predicted by the DVM method at the higher angles of attack for the s_m/D=1.25 configuration. In this study however, the normal force was slightly under-predicted by the DVM method for all configurations. At supersonic speeds the DVM method predicted the centre-of-pressure positions to be further aft compared to the presented CFD data at the relevant Mach numbers. In this study, at incompressible Mach numbers, the DVM method predicts the centre-of-pressure positions further forward compared to CFD.

The vortex positions predicted by the DVM method in reference [10] are poorly predicted compared to the CFD vortex positions above angles of attack of 6°. Similar results were obtained in this study as discussed in the previous section. The accuracy of the vortex position predictions tends to increase with increasing span to body diameter ratio. The loads are also predicted less accurately at the span to body diameter ratios above 1.25.

8 Conclusions

This study investigated the applicability of the DVM and FVM methods to predict the leeside flow for cruciform wing-body combinations with very low aspect ratio wings in the '+' configuration at incompressible speeds. The following can be concluded:

- Both the FVM and DVM methods predict the normal force with reasonable accuracy for the $s_m/D=1.25$ configuration. The centre-of-pressure is, however, only reasonably predicted at very low angles of attack (below 6°) by both methods.
- Despite the errors in the centre-of-pressure predictions, the FVM method showed better correlation at subsonic speeds than the supersonic predictions in reference [4].
- The FVM method decreases in accuracy at the higher span to body diameter ratios and is therefore not applicable at such configurations. The DVM method is more suitable at higher span to body diameter ratios.

9 References

[1] Tuling S, Dala L and Toomer C. Lee-side flow structures of very low aspect ratio cruciform wing-body configurations. *Journal of Spacecraft and Rockets*, Vol. 50, No. 6, pp 1134-1149, 2013.

[2] Tuling S., Dala, L. and Toomer C. Some compressibility effects on the lee side flow structures of cruciform wing-body configurations with very low aspect ratio wings. *Aerospace Science and Technology*, Vol. 29, No. 1, pp 373-385, 2013.

[3] Tuling S., Dala, L. and Toomer C. Two-dimensional potential method simulations of a body-strake configuration. *Journal of Spacecraft and Rockets*, Vol. 51, No. 2, pp 468-477, 2014.

[4] Tuling S., Dala, L. and Toomer C. An engineering method for very low aspect ratio cruciform wing-body configurations.*31st Applied Aerodynamics Conference, American Institute of Aeronautics and Astronautics*, AIAA-2013-2823, 2013.

[5] Allen H. J., Perkins E. W.A study of effects of viscosity on flow over slender inclined bodies of revolution. *NACA TR-1048*, 1951.

[6] Spahr J. R. Theoretical predictions of the effects of vortex flows on the loading, forces and moments of slender aircraft. *NASA TR R-101*, 1961.

[7] Mendenhall M.R. Predicted vortex shedding from noncircular bodies in supersonic flow. *Journal of Spacecraft and Rockets*, Vol. 18, No. 5, pp 385-392, 1981.

[8] Sacks A.H. Behaviour of vortex system behind cruciform wings – motions of fully rolled-up vortices. *NACA TN 2605*, 1952.

[9] Mendenhall M.R., et. Al. Vortex shedding from circular and noncircular bodies at high angles of attack. *17th Aerospace Sciences Meeting*, New Orleans, AIAA-79-0026, 1979.

[10] Tuling S. An Engineering method for modelling the interaction of circular bodies and very low aspect ratio cruciform wings at supersonic speeds. PhD Thesis, *University of the West of England*, 2012.

Acknowledgement

The author would like to place on record thanks to the Council for Scientific and Industrial Research (CSIR), Aeronautic Systems Competency, that has funded and supported this project.

Copyright Statement

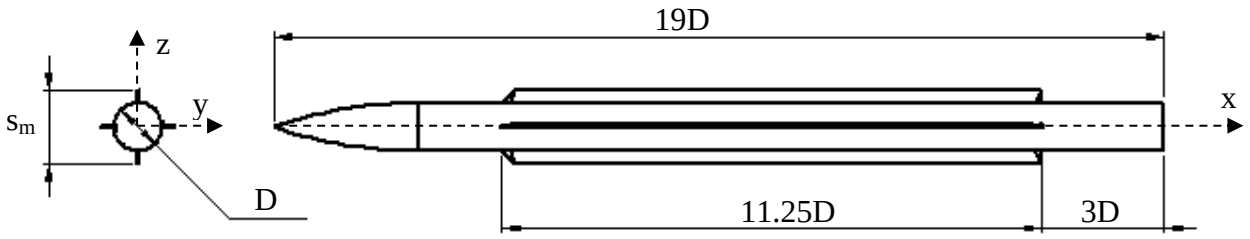

Fig. 1. Body-Strake Configuration

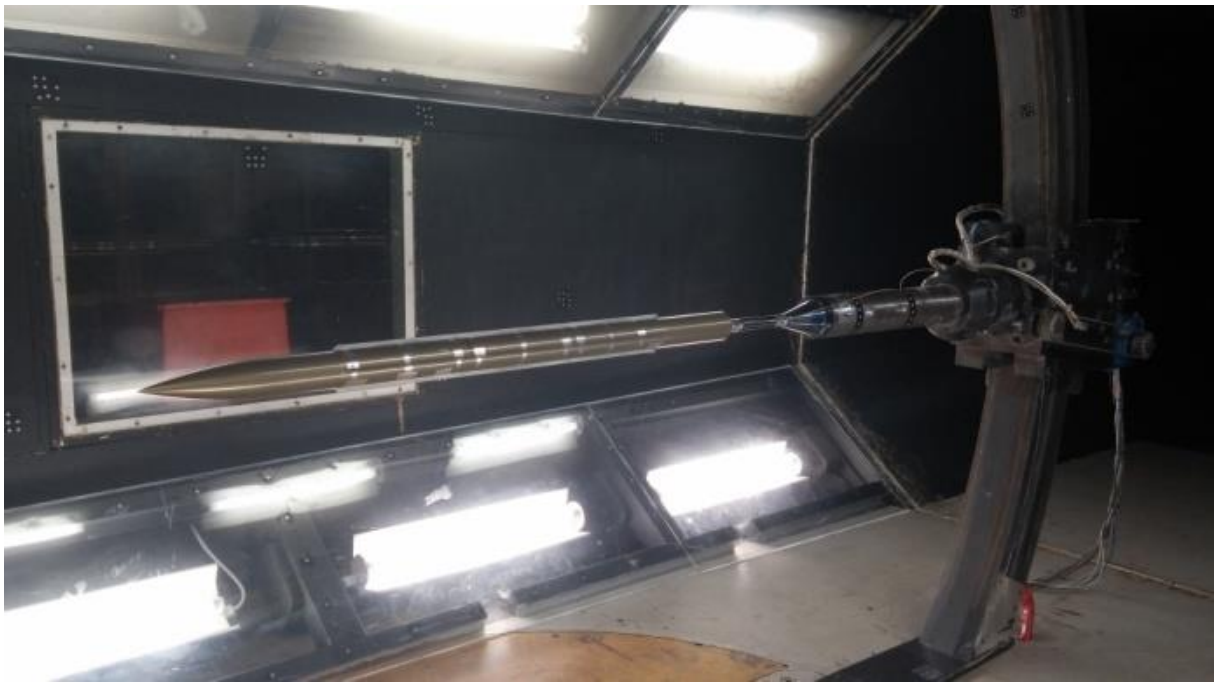

Fig. 2. Model Setup in LSWT

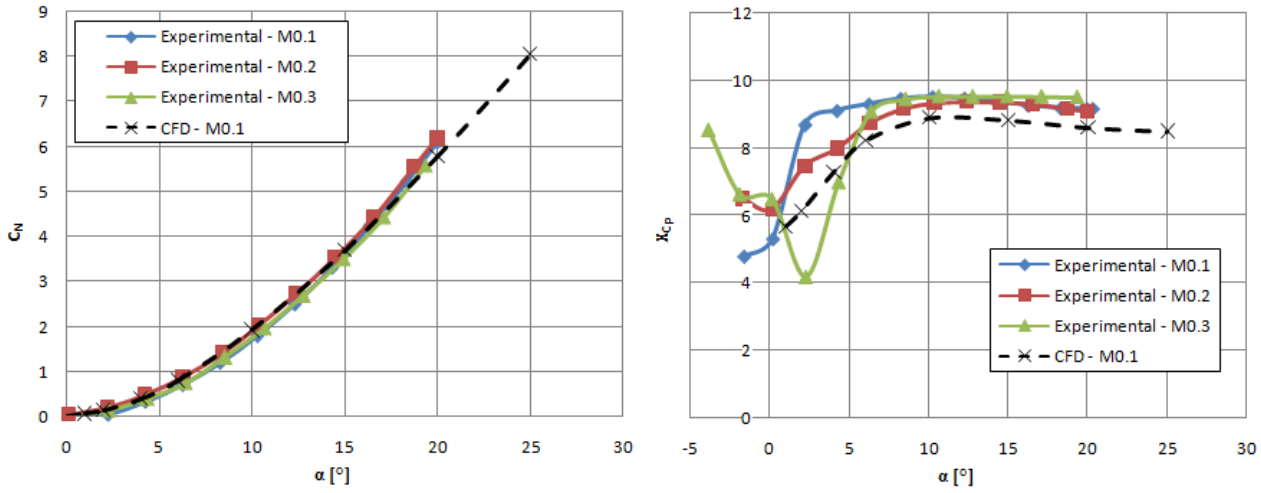

Fig. 3. Comparison of Experimental and CFD (a) Normal Force and (b) centre-of-pressure position for s_m/D=1.25

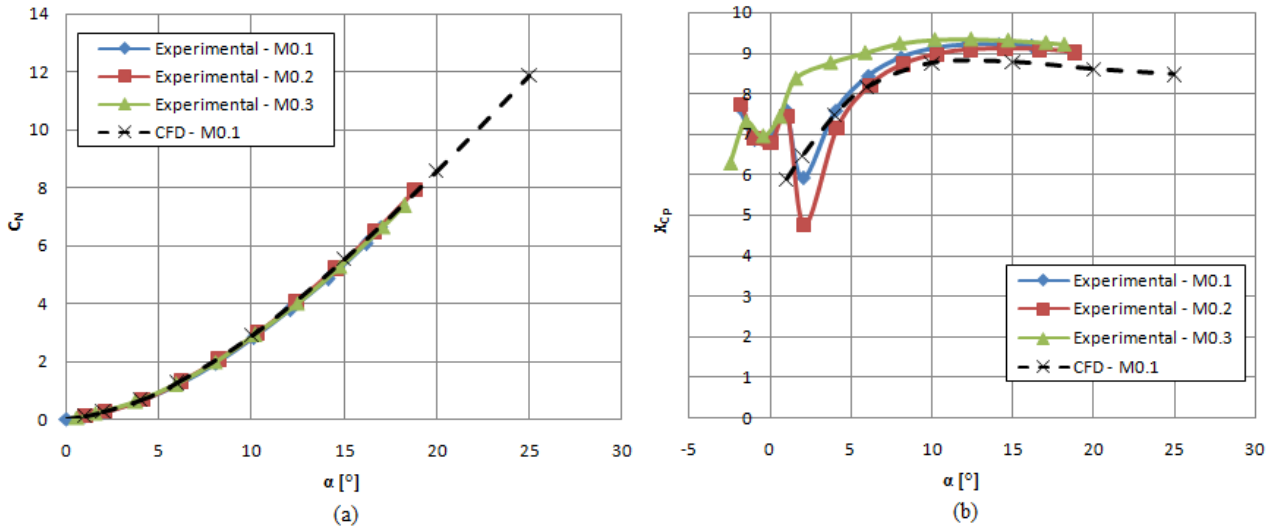

Fig. 4. Comparison of Experimental and CFD (a) Normal Force and (b) centre-of-pressure position for s_m/D=1.5

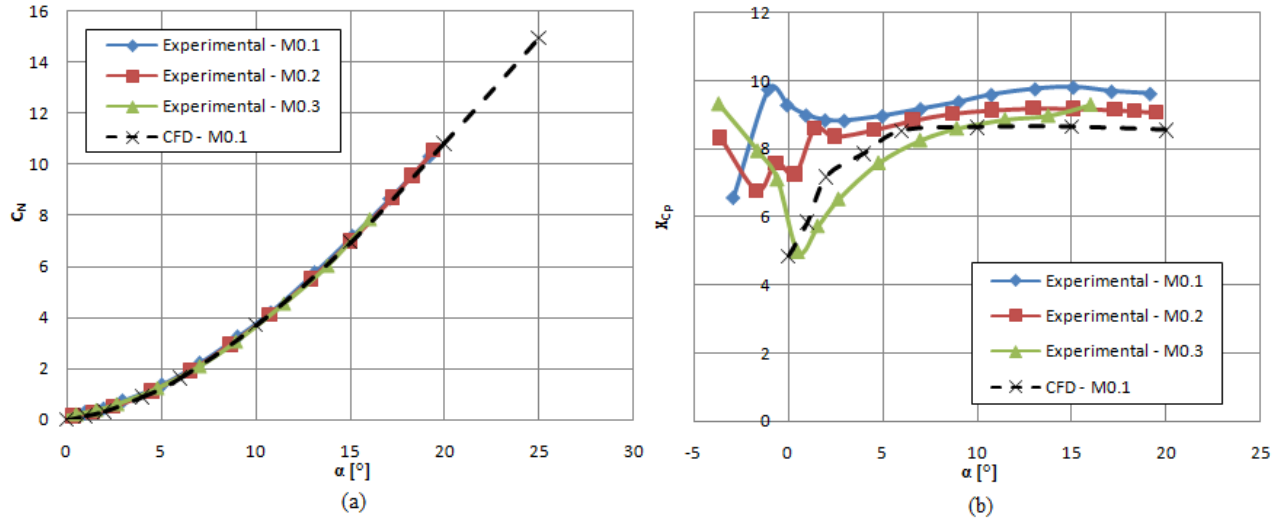

Fig. 5. Comparison of Experimental and CFD (a) Normal Force and (b) centre-of-pressure position for s_m/D=1.75

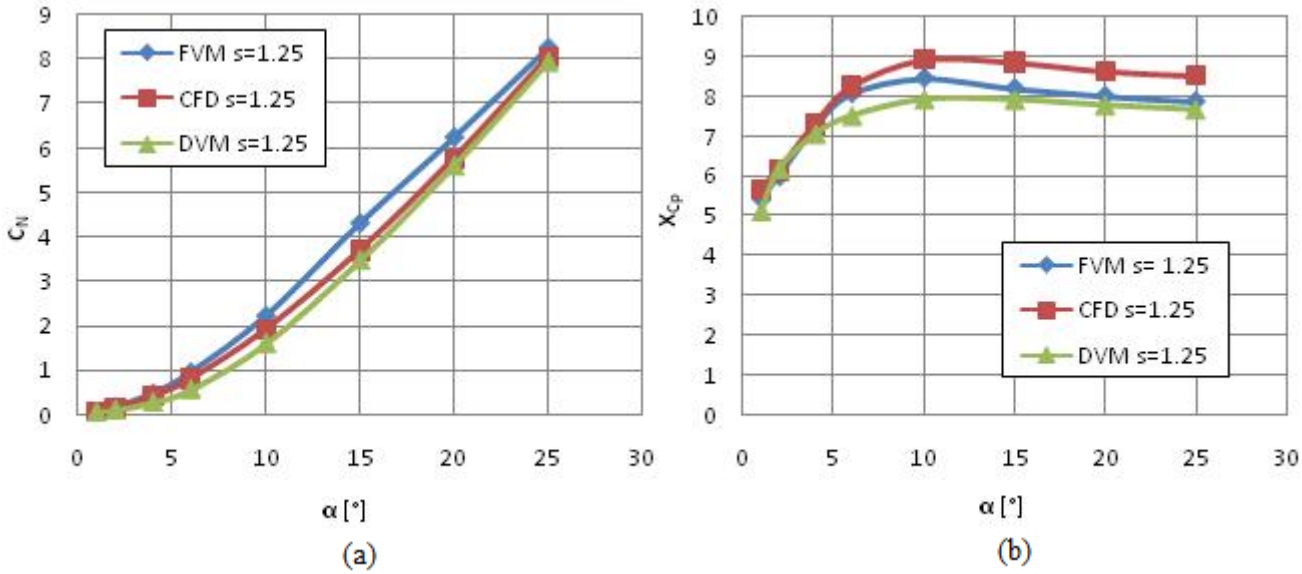

Fig. 6. Comparisons of (a) Normal Force and (b) Centre-of-Pressure for DVM and FVM Methods (s_m/D=1.25)

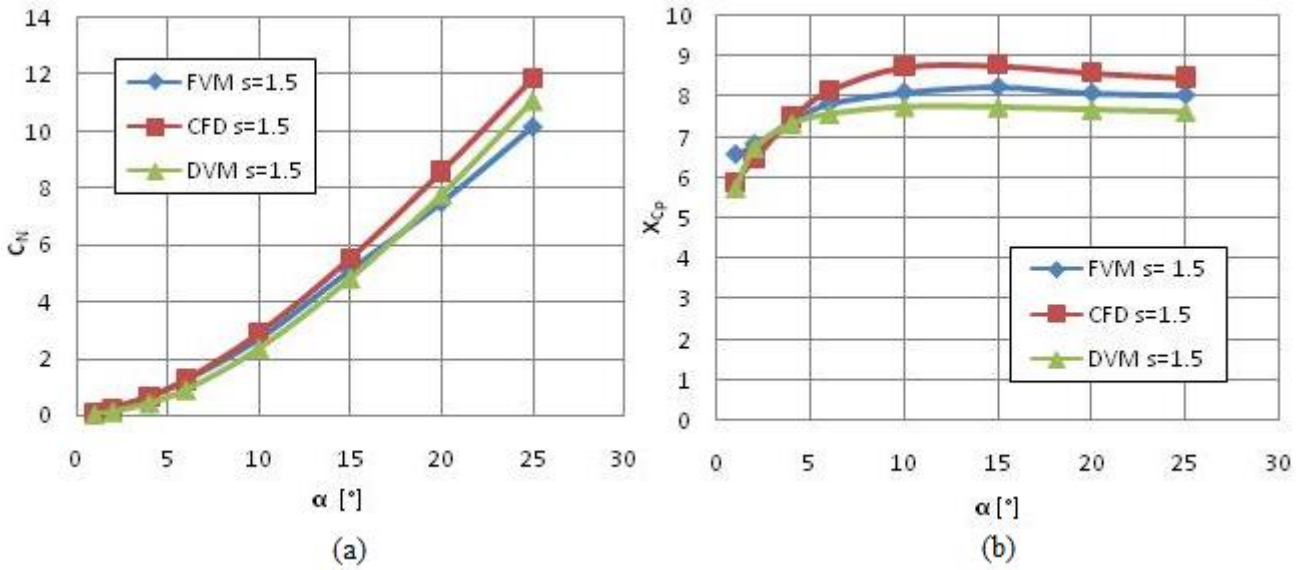

Fig. 7. Comparisons of (a) Normal Force and (b) Centre-of-Pressure for DVM and FVM Methods (s_m/D=1.5)

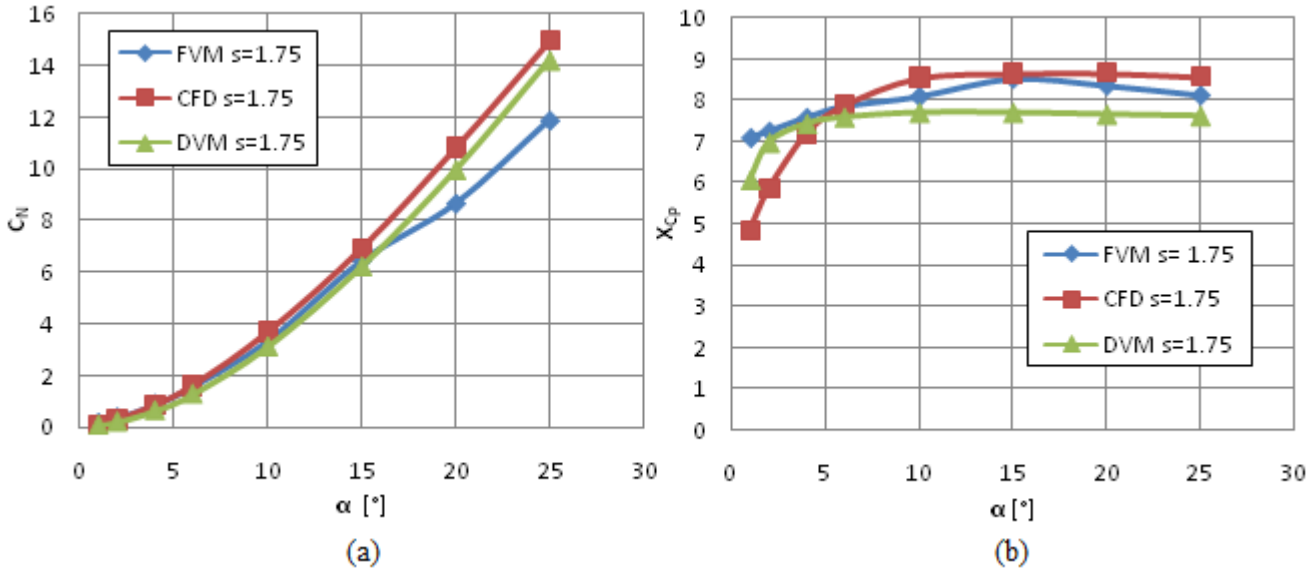

Fig. 8. Comparisons of (a) Normal Force and (b) Centre-of-Pressure for DVM and FVM Methods (s_m/D=1.75)

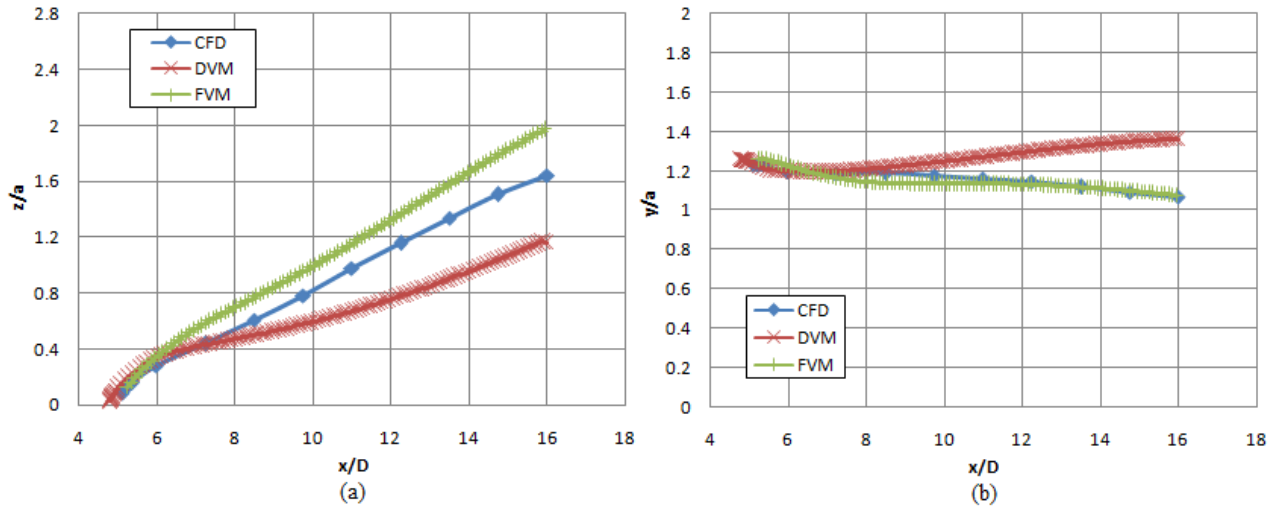

Fig. 9. (a) Vertical and (b) Lateral Vortex Position Comparison for s_m/D=1.25 at 10° angle of attack

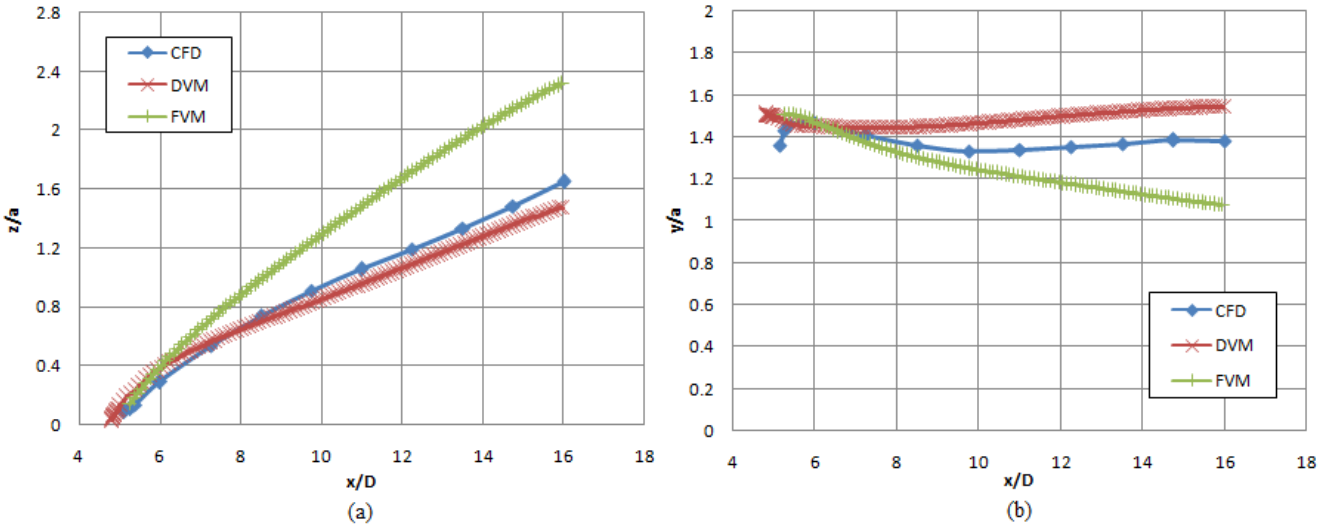

Fig. 10. (a) Vertical and (b) Lateral Vortex Position Comparison for $s_m/D=1.5$ at 10° angle of attack

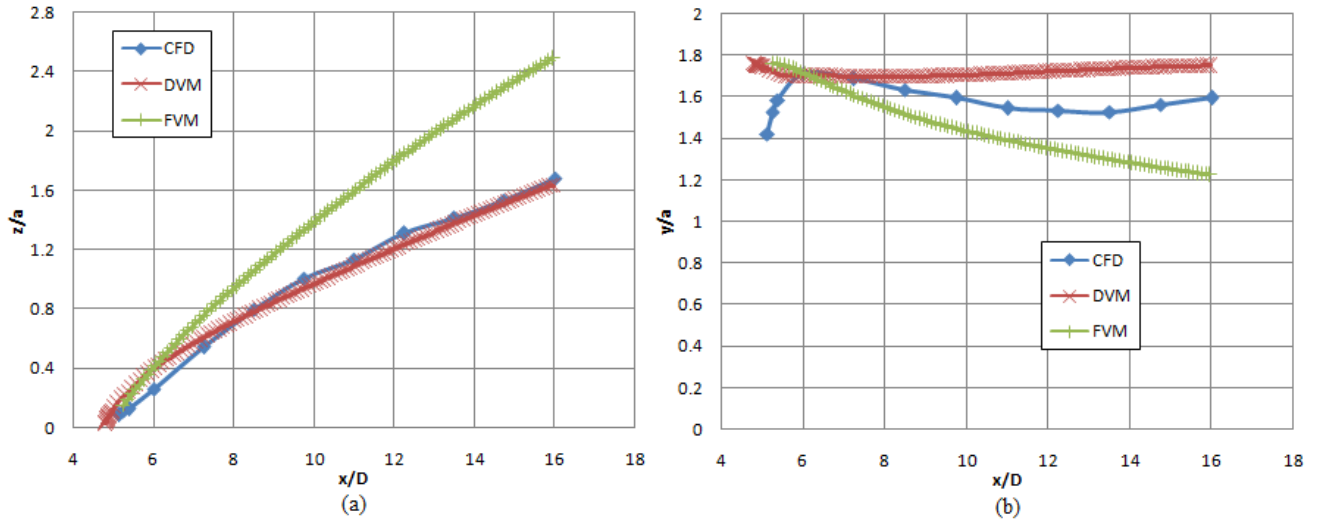

Fig. 11. (a) Vertical and (b) Lateral Vortex Position Comparison for $s_m/D=1.75$ at 10° angle of attack